2012

Structural, Magnetic, and Electron Transport Properties of MnBi:Fe Thin Films

Parashu Kharel
University of Nebraska-Lincoln, pkharel2@unl.edu

X. Z. Li
University of Nebraska-Lincoln, xli2@unl.edu

V. R. Shah
University of Nebraska-Lincoln

N. Al-Aqtash
University of Nebraska at Omaha, nalaqtash@unomaha.edu

K. Tarawneh
Princes Sumaya University for Technology (PSUT)

Structural, magnetic, and electron transport properties of MnBi:Fe thin films

P. Kharel,[1,2,a)] X. Z. Li,[2] V. R. Shah,[2] N. Al-Aqtash,[3] K. Tarawneh,[4] R. F. Sabirianov,[2,3] R. Skomski,[1,2] and D. J. Sellmyer[1,2]
[1]*Department of Physics and Astronomy, University of Nebraska, Lincoln, Nebraska 68588, USA*
[2]*Nebraska Center for Materials and Nanoscience, University of Nebraska, Lincoln, Nebraska 68588, USA*
[3]*Department of Physics and Astronomy, University of Nebraska, Omaha, Nebraska 68182, USA*
[4]*Department of Science and Humanities, Princes Sumaya University for Technology (PSUT) Amman, Jordan*

(Presented 1 November 2011; received 23 September 2011; accepted 4 November 2011; published online 1 March 2012)

The structural, magnetic, and electron transport properties of $Mn_{55-x}Fe_xBi_{45}$ (x = 0, 2, 4, 5, 8, 11, 13, 16) films prepared by multilayer deposition and annealing using e-beam evaporation have been investigated. Fe doping has produced a significant change in the magnetic properties of the samples including the decrease in saturation magnetization and magnetocrystalline anisotropy and increase in coercivity. Although the magnetization shows a smooth decrease with increasing Fe concentration, the coercivity jumps abruptly from 8.5 kOe to 22 kOe as Fe content changes from 4% to 5%, but the change in coercivity is small as the concentration goes beyond 5%. The temperature dependence of resistivity shows that the samples with low Fe concentration ($\leq$4%) are metallic, but the resistivity increases unexpectedly as the concentration reaches 5%, where the resistance increases with decreasing temperature below 300 K. First-principle calculations suggest that the observed magnetic properties can be understood as the consequences of competing ferromagnetic and antiferromagnetic exchange interactions between the interstitial atom and the rest of the MnBi lattice. © *2012 American Institute of Physics*. [doi:10.1063/1.3675615]

MnBi is one of the few ferromagnetic manganese compounds that has a Curie temperature well above room temperature[1] and has appreciable coercivity that increases with increasing temperature.[2,3] In thin films, MnBi shows a large room temperature magnetocrystalline anisotropy perpendicular to the film plane.[4] Because these properties are promising for permanent-magnet applications, MnBi has attracted much attention as a potential non-rare-earth material for permanent magnets.[3,5–7] Other interesting properties of this material in thin films include an extraordinarily large Kerr rotation,[8] high value of transport spin polarization,[9] and an unusual spin correlations leading to Kondo effect when doped with heavy and noble metals such as Pt and Au.[10,11] Recently, there have been efforts to improve the structural and magnetic properties of this material with the substitution of a third element, which has stimulated the current work. Here, we present our experimental investigations on the effect of Fe impurity on the structural, magnetic and electron transport properties of MnBi films.

Fe-doped MnBi films with a range of Fe concentrations were prepared on glass substrates using an e-beam evaporation system. The multilayer films were deposited at a base pressure of 6×10^{-9} Torr, and the substrate temperature of 125 °C. A thin layer of Bi was first deposited onto the hot glass substrate, and alternate layers of Mn and Fe were deposited on the Bi base-layer. The multilayer samples were annealed *in situ* after deposition in two steps: first at 290 °C for 2 h and then at 410 °C for 1 h before slowly cooled to room temperature. The elemental compositions of the samples were estimated from the deposition layer thicknesses. The data presented here were collected on the samples of thickness about 47 nm and atomic compositions of $Mn_{55-x}Fe_xBi_{45}$ (x = 0, 2, 4, 5, 8, 11, 13, 16) as determined by the energy dispersive x-ray spectroscopy (EDX). We used x-ray powder diffraction (XRD) and transmission electron microscopy (TEM) to investigate the crystal structure and the Quantum Design magnetic property measurement system (MPMS) was used to study the magnetic properties.

Figure 1 shows x-ray diffraction patterns of four representative samples with Fe concentrations 0%, 4%, 8%, and 13%. All $Mn_{55-x}Fe_xBi_{45}$ films are single phase MnBi with the hexagonal NiAs structure and are highly c-axis textured, but traces of unreacted Bi have been found in samples with higher Fe concentration. Although all the samples maintain c-axis texture, Fe substitution has produced significant change in the c-axis lattice parameter (c). The values of c were calculated from the positions of (002) reflections in the XRD patterns [see inset (a) of Fig. 1]. As shown in inset (b) of Fig. 1, the c-parameter increases systematically as Fe concentration increases up to 8% and then decreases with further increase in the amount of Fe. This suggests that Fe atoms occupy the MnBi lattice for low concentrations of Fe, but probably Fe separates out into clusters as the concentration exceeds 11%. Interestingly, the full width at half maximum (FWHM) of (002) Bragg peak has been found to decrease with increasing Fe substitution as seen from the rocking curves [see inset (c) of Fig. 1]. The decrease in FWHM with increase in Fe content may indicate that the mosaic blocks are getting oriented parallel to the film plane. This argument is partially supported by our TEM observation that $Mn_{55-x}Fe_xBi_{45}$ grows in rod-like crystallites for higher Fe concentration. The decrease in intensity can be attributed to the decrease in vertical coherence where interstitial occupation of the atoms may cause

a)Author to whom correspondence should be addressed. Electronic mail: pkharel2@unl.edu.

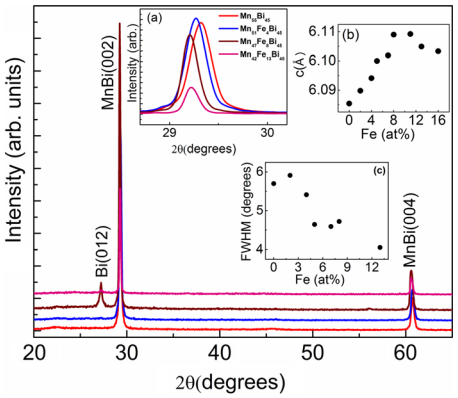

FIG. 1. (Color online) X-ray diffraction patterns of $Mn_{55-x}Fe_xBi_{45}$ (x = 0, 4, 8, 13) films. Inset (a) shows the close-up view of the most intense (002) peak. The Fe concentration dependence of the c-axis lattice parameters and the full width at half maximum (FWHM) of the rocking curves are shown in insets (b) and (c), respectively.

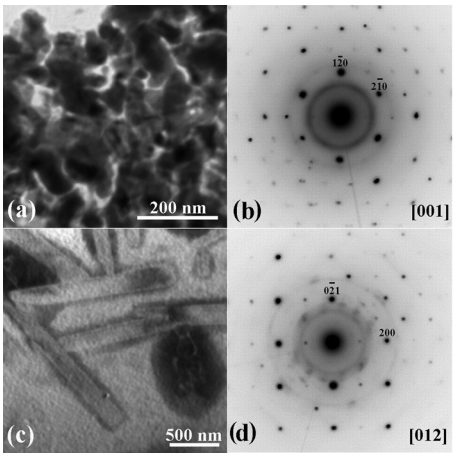

FIG. 2. TEM bright field images of the specimens prepared from $Mn_{55}Bi_{45}$ and $Mn_{50}Fe_5Bi_{45}$ films are shown in (a) and (c) and the corresponding SAED patterns are shown in (b) and (d), respectively.

some disorder in the lattice resulting in the loss of scattered intensity.

To better understand the effect of Fe doping on the crystal structure of MnBi, we have performed TEM studies on two sets of MnBi samples: one without Fe and the other with 5% Fe. The TEM specimens were prepared by mechanical polishing and ion-beam milling. We have found a significant change in the particle size and crystal structure of MnBi films due to Fe doping [Figures 2(a) and 2(c)]. The film without Fe is composed of small particles of size between 20 nm and 150 nm, whereas the sample with 5% Fe consists of 1 μm to 2 μm long rod-like structures. This is consistent with the XRD result that the width of the rocking curves in Fe doped samples decrease as Fe concentration increases. The selected area electron diffraction (SAED) pattern of $Mn_{55}Bi_{45}$ film agrees well with its XRD pattern confirming the hexagonal NiAs structure [Fig. 2(b)]. While the XRD patterns of Fe substituted samples are also consistent with the NiAs structure, the SAED pattern of the 5% Fe substituted sample is slightly different and shows an orthorhombic distortion in the crystal lattice [Fig. 2(d)]. MnBi in the high-temperature phase, where a fraction of Mn atoms occupy the interstitial sites, crystallizes in the distorted NiAs or orthorhombic structure.[4] This suggests that there is a partial occupation of interstitial sites by Mn or Fe atoms.

We have found a significant change in the magnetic properties of MnBi films due to Fe substitution. The out-of-plane M(H) hysteresis loops are almost rectangular for all the films, but the samples with higher Fe concentrations ($\geq$11%) show a signature of mixed phase. Figure 3 illustrates the room-temperature M(H) loops of some selected samples, and the inset shows the loop of the sample with highest Fe concentration of 16%, which suggests that the sample contains exchange-coupled hard and soft phases. We believe that the Fe atoms that are not incorporated into MnBi lattice have soft magnetic properties in these films. Figure 4 illustrates the effect of Fe substitution in magnetization, anisotropy energy, and coercivity of MnBi films. At room temperature, the saturation magnetization (M_s) of MnBi film is 580 emu/cm^3; this decreases monotonically with increasing Fe concentration and reaches 154 emu/cm^3 as Fe concentration reaches 11%. Beyond 11%, M_s shows a sluggish increase perhaps due to the presence of small amount of unreacted Fe in the films. The room-temperature anisotropy energy ($K_u = K_1 + K_2$) also shows similar dependence on Fe concentration where K_u decreases from 1.6×10^7 to 3.6×10^6 ergs/cm^3 as Fe concentration increases from 0 to 11% (see the inset of Fig. 4). The anisotropy constants K_1 and K_2 were calculated using $E = K_1 \sin^2\theta + K_2 \sin^4\theta$ - H $M_s \sin\theta$ and the Sucksmith–Thompson method[12] where E is the energy density, M_s is the saturation magnetization, and θ is the angle between easy axis and magnetization.

To understand the observed structural and magnetic properties of Fe substituted MnBi films, we performed first-principle calculations of 3.125% Fe doped MnBi in a $Mn_{15}Fe_1Bi_{16}$ supercell of 32 atoms using the projector augmented wave method,[13,14] within a Perdew-Burke-Ernzerhof generalized gradient approximation[15] of the density functional theory. The simulations were performed using periodic boundary conditions. We used $6 \times 6 \times 6$ k-point sampling, and the atomic positions of all atoms in the unit cells were relaxed using the Hellmann–Feynman scheme till forces were less than 0.005 eV/Å. We have evaluated the change in total energy and magnetization of the system as Fe occupies various possible lattice sites. We considered three structural arrangements: (i) ordered structure where Fe replaces one of the Mn in the regular lattice site, (ii) disordered structure

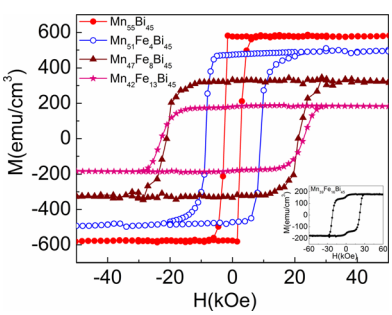

FIG. 3. (Color online) The out-of-plane magnetization of $Mn_{55-x}Fe_xBi_{45}$ (x = 0, 4, 8, 13) films as a function of magnetic field measured at room temperature. The inset shows the room temperature M(H) loop of $Mn_{39}Fe_{16}Bi_{45}$ film.

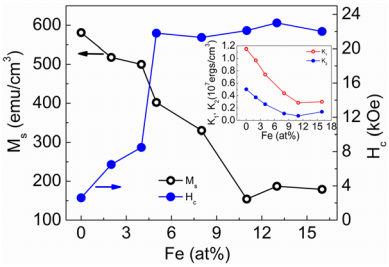

FIG. 4. (Color online) The room temperature saturation magnetization (scale on the left) and coercivity (scale on the right) as a function of Fe concentration for $Mn_{55-x}Fe_xBi_{45}$ films. Inset shows the change in anisotropy constants K_1 and K_2 of MnBi films as Fe concentration increases from 0% to 16%.

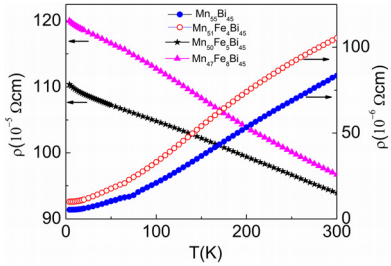

FIG. 5. (Color online) Temperature dependence of electrical resistivity of four representative $Mn_{55-x}Fe_xBi_{45}$ samples with x = 0, 4, 5, and 8.

where Fe occupies interstitial site with one of the lattice sites empty, and (iii) disordered structure where Fe replaces Mn in the lattice site and Mn occupies the interstitial site. We have examined both ferromagnetic (FM) and antiferromagnetic (AFM) couplings between the interstitial and regular lattice moments. Similar investigation where MnBi is doped with a heavy and noble element can be found elsewhere.[10]

Table 1 summarizes the calculated values of total energy and magnetization for the aforementioned structural arrangements along with the values for undoped MnBi. We have found that the total energy has smallest value for structure (i) where the substituted iron shows FM interaction with the rest of the Mn lattice. But the magnetization decrease of 2.2% in this case does not agree with our experimental result. However, the magnetization decrease of 15.5% in structure (iii), where interstitial Mn shows AFM coupling with the rest of the magnetic moments (AFM2 in the table), compares well with the magnetization decrease of 13% observed experimentally for 3% Fe doping. This suggests that the magnetic structures in our samples are more complex than the one considered in the calculation.

The coercivity (H_c) of a permanent magnet is expected to scale roughly with anisotropy field given by $H_A = 2K_1/M_s$. However, in binary alloys with impurity doping, the defect structure of the material plays an important role in determining the coercivity. In our case, the jump at 5% is probably caused by domain wall pinning at crystalline inhomogeneities that start to form around this concentration. The coercivity and magnetization plateau above 11% Fe indicate a phase separation between hard and soft phases. In this region, the coercivity is determined by the magnetization and anisotropy of the hard phase, and there is little change in the hysteretic behavior (see Fig. 4).

In addition to the structural and magnetic properties, we have investigated the electron-transport properties of the films. As shown in Fig. 5, the temperature dependence of resistivity between 4 K and 300 K shows that the films with low Fe concentration (up to 4%) are metallic ($d\rho/dT > 0$), but the resistivity changes dramatically as the concentration increases beyond 4%. Below 300 K, a monotonic increase in the resistance of the $Mn_{55-x}Fe_xBi_{45}(x \geq 5)$ films has been observed with decreasing temperature ($d\rho/dT < 0$). Because we did not find a significant change in the electronic structure due to Fe doping as seen from the first-principle calculations (not shown), we believe that the large change in resistivity behavior of samples having high Fe concentration ($x \geq 5$) is due to the change in the granular structure of the films as shown in Fig. 2(c).

In summary, we have investigated the structural, magnetic, and electron-transport properties of MnBi films doped with a wide range of Fe concentrations and found an interesting correlation between Fe content and the structural, magnetic and electron transport properties. Fe doping has produced a significant change in the magnetic properties of the samples including the decrease in saturation magnetization and magnetocrystalline anisotropy and increase in coercivity. We explain these effects as the consequences of the competing ferromagnetic and antiferromagnetic exchange interactions of the interstitial atoms with the rest of the MnBi lattice.

TABLE I. Total energies (E_{tot}) and magnetizations (M) per unit cell of 32 atoms. FM and AFM correspond to the parallel and antiparrell alignment of Fe moment with the rest of the Mn moments. AFM2 corresponds to a special situation where Fe moment aligns parallel to the lattice Mn and antiparallel to the interstitial Mn moment.

		E_{tot} (eV)	M (μ_B)
$Mn_{16}Bi_{16}$		−200.1808	56.30
$Mn_{15}Fe_1Bi_{16}$	FM	−198.86476	55.06
Structure (i)	AFM	−198.49024	51.33
$Mn_{15}Fe_1Bi_{16}$	FM	− 198.79200	53.76
Structure (ii)	AFM	−198.43747	50.66
$Mn_{15}Fe_1Bi_{16}$	FM	−198.22034	52.93
Structure (iii)	AFM1(Fe↓, Mn↓)	−197.8708	41.97
	AFM2(Fe↑, Mn↓)	−198.3034	47.57

This research is supported by NSF MRSEC (Grant No. NSF-DMR-0820521) (P.K., R.F.S., N.A., K.T.), ARPA-E (DE-AR0000046, Subward No. 22101) (D.J.S., R.S.), ARO (Grant No. W911NF-10-2-0099) (X.Z.L., V.R.S.), and NCMN (Central Facility support). We would like to thank Pavel Lukashev for useful discussions.

[1]R. R. Heikes, Phys. Rev. B **99**, 446 (1955).
[2]U. Rüdiger and G. Güntherodt, J. Appl. Phys. **88**, 4221 (2000).
[3]J. B. Yang *et al.*, J. Phys.: Condens. Matter **14**, 6509 (2002).
[4]T. Chen and W. E. Stutius, IEEE Trans. Magn. **10**, 581 (1974).
[5]S. Cao *et al.*, J. Appl. Phys. **109**, 07A740 (2011).
[6]J. B. Yang *et al.*, Appl. Phys. Lett. **99**, 082505 (2011).
[7]Y. Liu *et al.*, Phys. Rev. B **72**, 214410 (2005).
[8]G. Q. Di *et al.*, J. Magn. Magn. Mater. **104**, 1023 (1992).
[9]P. Kharel *et al.*, Phys. Rev. B **83**, 024415 (2011).
[10]P. Kharel *et al.*, Phys. Rev. B **84**, 014431 (2011).
[11]P. Kharel *et al.*, J. Appl. Phys. **109**, 07B709 (2011).
[12]R. Skomski and J. M. D. Coey, *Permanent Magnetism* (IOP, Bristol, 1999).
[13]P. E. Blöchl, Phys. Rev. B **94**, 17953 (1994).
[14]G. Kresse and D. Joobert, Phys. Rev. B **59**, 1758 (1999).
[15]J. P. Perdew *et al.*, Phys. Rev. Lett. **77**, 3865 (1996).